A new method to image detailed Moho feature based on acoustic steepest-descend full waveform inversion

Shizhuo Mao [1], Xiaofeng Jia [3] and Lianxing Wen [2, 1]

1 Laboratory of Seismology and Physics of Earth's Interior, School of Earth and Space Sciences, University of Science and Technology of China
2 Department of Geosciences, Stony Brook University
3 University of Science and Technology of China

Email: mao@mail.ustc.edu.cn

Stony Brook University

NS13A-0007

1. Introduction

The detailed Moho features, such as its undulation and sharpness, are important in the understanding of regional tectonics. Several methods are used in imaging Moho and its surrounding structure. The receiver function method helps build Moho image, yet the imaging result is often not detailed because of the low frequency band. Surface wave tomography shows fine velocity structure in the crust, while the Moho imaging is not so clear due to the poor sensitivity of the dispersion curve to a certain velocity interface. Joint inversion methods based on receiver function or surface wave tomography cannot solve the problems, either. Full-waveform inversion (FWI), however, helps build clear Moho image because All types of waves in the seismogram including wide-angle reflections, multiples, are used in the optimization.

We develop a new method based on the acoustic steepest descend full-waveform inversion (FWI) to image detailed Moho features with Moho-reflected shear wave (SmS).

2. Theory and Method

In steepest descend FWI methods, the descend direction image is calculated by cross-correlation between the first-order time derivative of forward-modeling wave field from sources and time-reversal wave field of waveform residuals from receivers.

As known, FWI is an ill-posed problem, which means that a large number of models matches the data. In the steepest-descend FWI algorithm, this ill-posed problem occurs because of the sensitivity difference to different depth or regions of the descend direction (large sensitivity around the velocity interfaces), leading to a final inversed model differing significantly from the 'real' model. However, based on seismic interferometry and migration theory, the descend-direction image includes information of velocity structures, especially the location and shape of the velocity interfaces. It indicates that we can constrain and change the depth and shape of Moho based on the descend direction kernel, instead of changing the model velocity in the inversion.

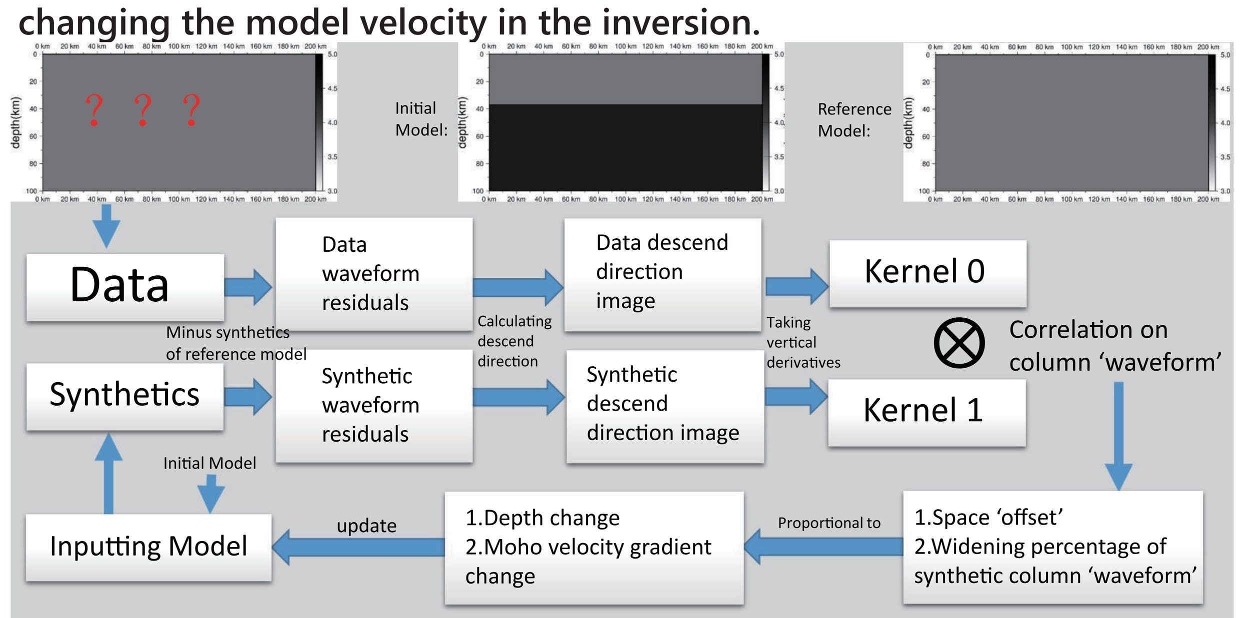

Fig. 1 Procedures of the new method. Waveform residuals are that from data/synthetics and the synthetics from the reference model. The reference model is also used for forward/backward wave field calculation in correlation.

In the new method, we build a reference model with clear crustal velocity structure and no Moho An initial model is obtained by adding a flat and sharp Moho to the reference model. Two descend-direction kernels are then calculated - The first kernel (Kernel-1) is calculated by correlating the forward wave field from a point source and the reverse-time propagation of the synthetic waveform for initial model as the backward wave field, and then taking its vertical derivative. In calculating the second kernel (Kernel-0), the backward wave field is built from the reverse time propagation of the data.

In each iteration, we estimate the depth and sharpness change of the Moho from the normalized cross-correlation between the 'waveform' of each column trace of the vertical derivative image of two descend-direction kernels. We define depth change as the 'space offset' (time difference) of the correlation, and sharpness change is set proportional to the widening percentage of the column 'waveform' from vertical derivative of Kernel-1 that corresponds to a normalized cross-correlation maximum with vertical derivative of Kernel-0. We then build new models based on different coefficient of the widening percentage and select the model with the minimum waveform residual as the inputting model in next iteration. As a result, the descend-direction kernel of the final model gets closest to Kernel-0, indicating that the synthetic for the inversed model has smallest waveform residual (especially traveltime and phase width) with the data.

3. Synthetic Tests

Synthetic tests are performed on two typical models to test the sufficiency of the new inversion method in imaging both topography and velocity sharpness of the Moho All synthetics are constructed with an acoustic finite-difference algorithm over epicenter distance in 200km, and an explosion point source of Gaussian wavelet. Results show fine detailed image for both gradient and undulating Moho interface.

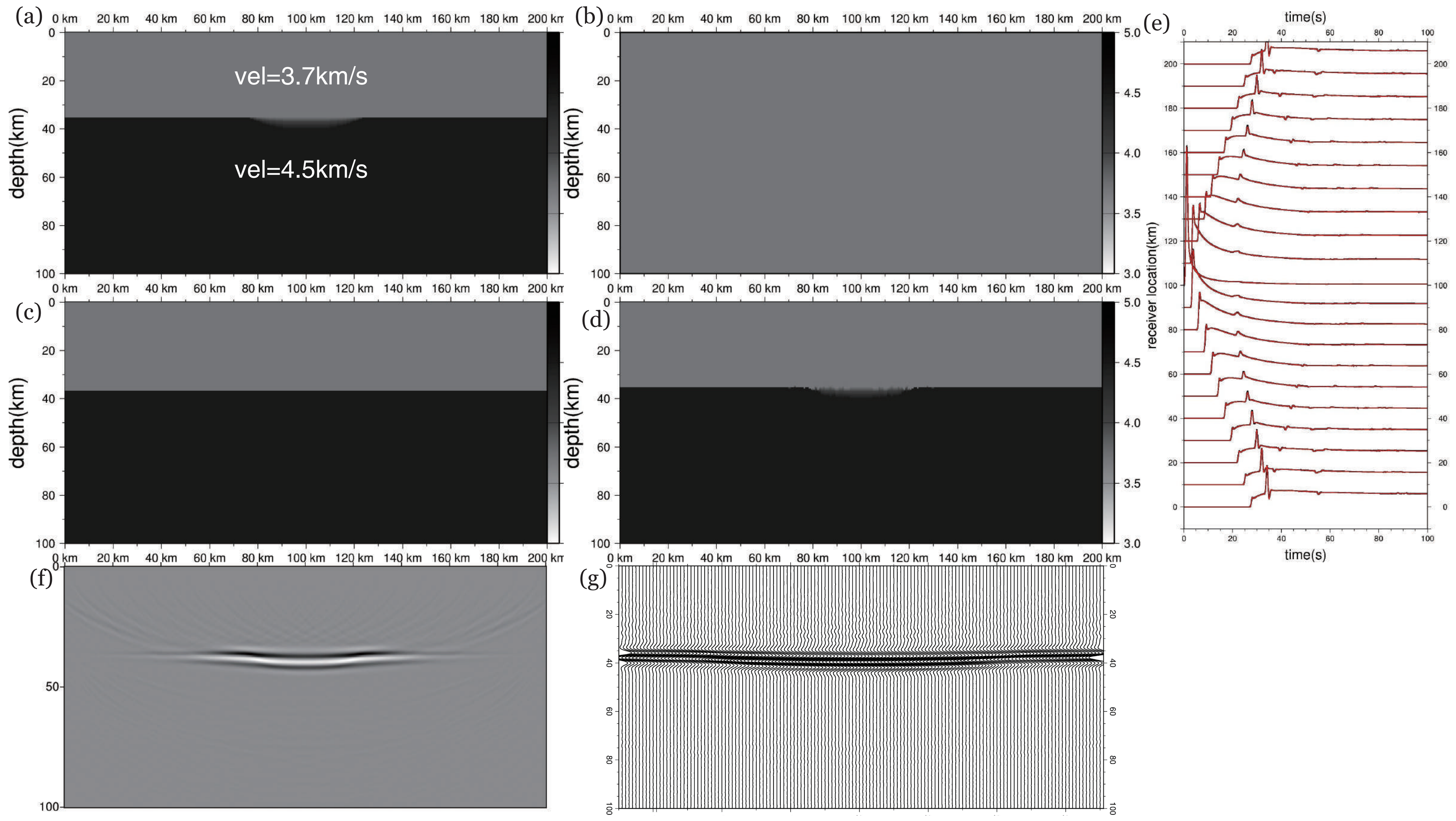

Fig. 2 Synthetic tests on an gradient Moho model. A gradient Moho velocity zone is set at the depth from 35km to 40km, in other regions of the model, Moho depth is set as 35km (a). A uniform model with velocity the same as that in the crust is set as the reference model (b), while a 1-d model with Moho at 37km is set as the initial model (c). Clear Moho image can be see in the calculated Kernel-0(f) and the corresponding column 'waveform' (g). Inversion result (d) shows fine imaging of both Moho depth and the shape and gradient of the gradient velocity zone, proved by the comparison of the waveform (e) with source at x=100km(red: synthetics; black: data).

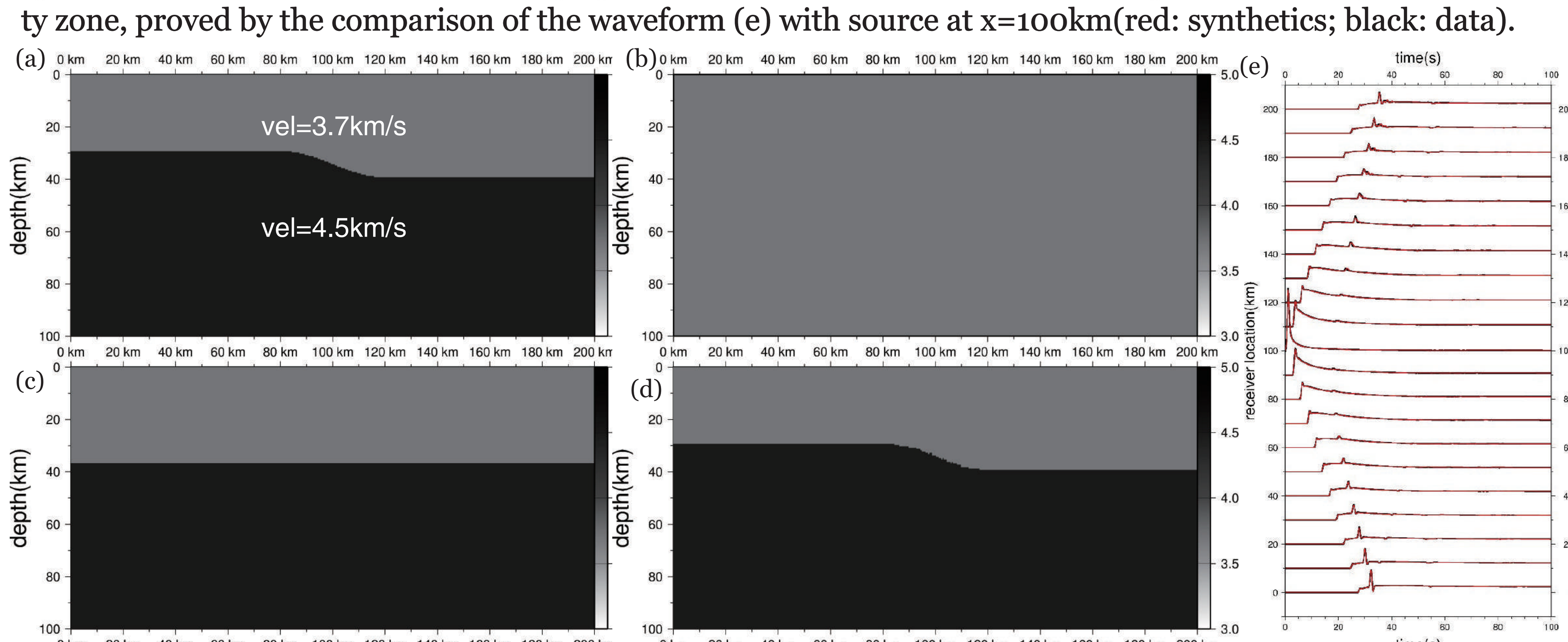

Fig. 3 Synthetic tests on a sharp Moho with large topography. A Moho depth change is set at 90-110km, with depth changing from 30km to 40km (a). The same as above, a uniform model with velocity the same as that in the crust is set as the reference model (b), while a 1-d model with Moho at 37km is set as the initial model (c). Inversion result (d) also shows good recovery of both Moho depth and the topography of the gradient velocity zone, proved by the comparison of the waveform (e) with source at x=100km.

4. Data Application test on NCISP6, NE China

To do a data application test, we combine the new method with ambient seismic noise cross-correlation (ASNCC) to test the ability to inverse Moho structure of the new method. Each station can be viewed as a virtual source with respect to ASNCC, which helps build numbers of reflection profiles.

We select NCISP6 Array in NE China (from station NE24 to station NE60) to do the test because geophones in this array is almost equally spaced. By stacking noise cross correlograms over 6 months and a bandpass filter at 0.2-0.5Hz, we build noise correlation profiles which include both body wave reflections (SmS) and Rayleigh phases with reference station from NE24 to NE60.

Several steps are carried out on noise correlation profiles before the inversion. Station pairs with distance <100km or >400km are removed because of strong Rayleigh waves and no sign of existence of SmS. Possible Rayleigh waves (with velocity <3.2km/s)

Fig. 4 NCISP6 Array. We selected stations from NE24 to NE60 (blue box), covering 600km. The distance between neighboring stations is 16.6km ± 0.1km.

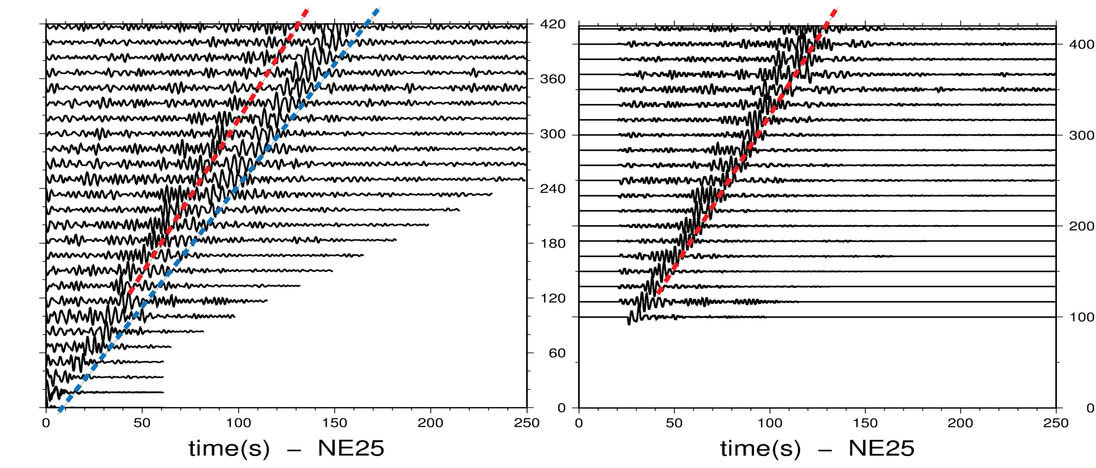

Fig. 5 An example profile with reference station at NE25. Both clear body wave reflections (SmS, or other multiples, red dashed line) and Rayleigh waves (blue dashed line, with group velocity within 2.6~3.2km/s) can be see in the cross correlogram profile (a). After suppression of Rayleigh phases and removal of other large amplitudes in the correlation, a profile for inversion (b) with clear time-derivative body wave (red dashed line) is obtained.

are suppressed to avoid impact on the kernel calculation. Waveform at 0~20s is also removed.

To do inversion using noise correlation profiles, we focus on the depth and topography of Moho based on a simple reference model instead of gradient Moho velocity gradient because the source time function is unknown.

A ricker-wavelet point source (with main frequency at 0.32Hz) is used in forward wavefront modeling, correlating with reverse-time propagation of the modified noise correlation profile. The calculated data kernel (Kernel-0), shown in Fig.6c (Red dashed-line frame), indicates the existence of a velocity interface at about 28-40km.

We build a uniform velocity model as the reference model (Fig.6b), and a two-layer 1-d model as the initial Model with Moho interface at 28km (Fig.6a) to do the inversion. Relative time differences between synthetics and data are considered in the iterations in order to make sure that SmS in data and synthetics have the same traveltime for the same distance. The final model (Fig.7d)shows fine recovery in regions where data kernel supplies clearer Moho image.

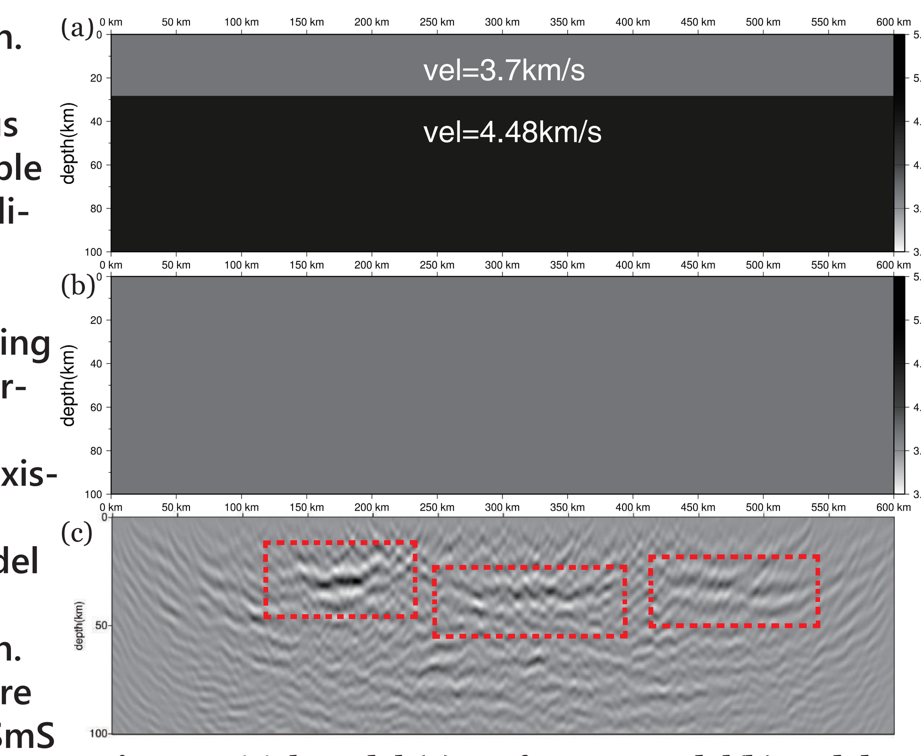

Fig. 6 Initial Model (a), Reference Model(b) and data kernel (Kernel-0, c). The red dashed-line frames show the existence of Moho at the depth 28-40km.

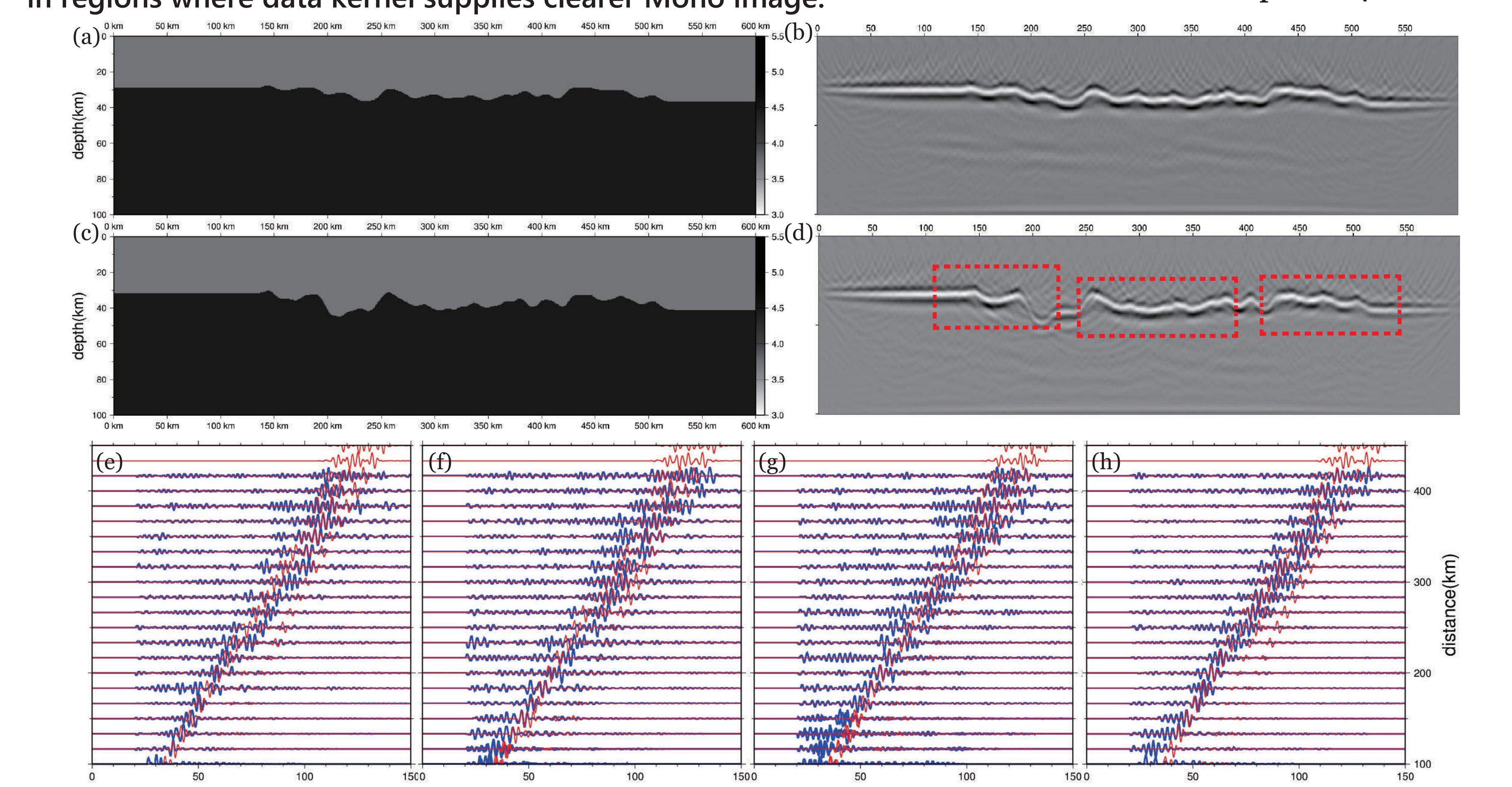

Fig. 7 Models, kernels and waveform comparison in the inversion. Traveltime difference between synthetics and data indicates a global smaller Moho depth for the model after 1st iteration(a, Kernel-1: b), while after three iterations, kernel from synthetics (d) gives better recovery compared to Kernel-0 (red dashed-line frames). Synthetics waveform examples for the model (c) after 3 iterations (e~h) show that the time period where SmS and other multiples exist are consistent with data for most station pairs.

5. Conclusions and outlook

1. We develop a new method based on acoustic steepest descend FWI to image detailed Moho features. By taking vertical derivatives of the descend direction image as the kernel and doing cross-correlation between synthetic kernel (Kernel-1) and data kernel (Kernel-0) iteratively, the new method constrain Moho topography and sharpness instead of constrain velocity change. Synthetic tests show fine imaging result for both topography and gradient Moho model.

2. We combine the new inversion method with ambient noise cross-correlation to test the capability of the new method to image Moho in 'aseismic' areas. An inversed Moho with similar waveform travel-time and kernel compared to the data is obtained based on a simple 2-layer model.

3. This method provides a prototype of imaging Moho and other complex structure in the crust in an acoustic (SH) system. Although result of this new method depend extremely on the crustal velocity structure, which means different reference models lead to totally different inversion results, this requirement of background crustal velocity structure may be satisfied with the help of surface waves in the P-SV system in the future studies.

Acknowledgment

We gratefully appreciate the IGG-CAS and IRIS for the high-quality NCISP6 Array data.